Acta Astronautica Vol. 12, No. 10, pp. 861–869, 1985
Printed in Great Britain.

0094–5765/85 $3.00 + .00

PERTURBATION SOLUTION OF ATTITUDE MOTION UNDER BODY-FIXED TORQUES†

JOZEF C. VAN DER HA‡
European Space Operations Centre (ESA), Robert-Bosch-Strasse 5, 6100 Darmstadt, FRG

(*Received* 28 *February* 1985)

Abstract—Approximate analytical solutions are established for the attitude rates and angles of a rigid body subjected to a constant body-fixed torque. The perturbation solutions obtained are valid for any arbitrary inertia parameters. The small parameter is defined as the ratio between representative transverse rotation rate and the spin or scan rate. The results should be useful for quickly evaluating the attitude response of a spin-stabilised or scanning spacecraft to a variety of torque inputs. The applicability of the theory is illustrated by means of practical examples such as the spin-down due to rate coupling of ESA's GEOS spacecraft and the prediction of the attitude drift of the HIPPARCOS satellite during payload initialisation. Furthermore, the compact first-order results should be suitable for implementation in on-board manoeuvre or attitude control software.

1. INTRODUCTION

The attitude evolution of a spacecraft under various torques has been studied extensively over the past few decades. Usually a great deal of numerical simulations are required until the attitude response and control characteristics are understood in sufficient detail. Analytical models can be of great help in obtaining a qualitative understanding of the dynamical features involved. In the case of axisymmetric spinning satellites a fairly complete theory exists, at least for constant body-fixed torque components. The internal ESA report of Janssens[1] gives a good practical survey on the results available.

The classical literature (i.e. before the advent of artificial satellites) contains many special cases of rigid body motion which unfortunately are hardly ever directly applicable to practical satellite problems. From an historical point of view the book by Leimanis[2] and the papers by Grammel[3] are of interest.

In the near future, on-board capabilities with regard to attitude control autonomy are expected to evolve rapidly. The on-board autonomy would benefit considerably from the availability of compact analytical models for attitude evolution under various torques. As an important step in this direction Longuski[4] presented an analytical model for the attitude evolution of a near-symmetric spacecraft under a constant body-fixed thrust. The results are shown to be of interest for autonomous manoeuvering of the GALILEO spacecraft.

The present paper aims at providing compact representations for the attitude evolution of spacecraft with arbitrary inertia parameters under constant body-fixed torques. Apart from being of interest for future on-board attitude control implementation and manoeuvre planning the models are also useful for more traditional simulation and evaluation tasks.

The analysis makes use of perturbation theory which has found widespread application in orbit motion studies but for no obvious reason has never had a similar impact on attitude dynamics problems. As practically all satellites have one designated spin or scan axis it appears natural to take the ratio of a representative transverse rotation rate and the spin or scan rate as the small perturbation parameter. This condition can be shown to be roughly equivalent to attitude motion with a small nutation angle.

The analytical results are illustrated to two actual applications. First, the little-known spin-down effect induced by rate coupling during axial thrust is derived from the theory. This spin-down can well have catastrophic consequences as was vividly demonstrated by the GEOS dynamic experiment[5]. The second application concerns the attitude drift prediction of ESA's astrometry satellite HIPPARCOS during its initialisation phase. This slowly scanning satellite is perturbed by a torque due to a gyro reaction to the imposed scanning. The attitude drift prediction is of vital importance for assessing the feasibility of the separation of the star patterns observed in the two telescopes combined fields of view. This in turn is necessary for obtaining full three-axis attitude knowledge.

2. ATTITUDE RATE EVOLUTION UNDER CONSTANT BODY-FIXED TORQUE

2.1 *Equations of attitude rate evolution*

A body-fixed principal coordinate frame x, y, z is introduced such that the z-axis points along the positive spin axis direction (or along the axis with largest nominal rotation rate in the case of scanning motion). The equatorial principal axes are oriented such that the moment of inertia I_y is larger than I_x or arbitrary if they are equal.

The inertia parameters:

$$k_x = (I_z - I_y)/I_x; \quad k_y = (I_z - I_x)/I_y; \quad k_z = (I_y - I_x)/I_z \quad (1)$$

are introduced. It can be seen that both k_x and k_y are

†Paper presented at 35th Congress of the International Astronautical Federation, Lausanne, Switzerland, 8–13 October 1984.

‡Senior Analyst.

positive in the case that z is the major axis of inertia and that both are negative if z is the minor inertia axis. It may be recalled that spin around an intermediate axis of inertia is not physically possible. By virtue of definition k_z is nonnegative.

Euler's equations of attitude motion describe the evolution of the angular body rates ω_x, ω_y, ω_z under general torque components T_x, T_y, T_z:

$$\begin{aligned} \dot{\omega}_x + k_x\omega_z\omega_y &= T_x/I_x, \\ \dot{\omega}_y - k_x\omega_z\omega_x &= T_y/I_y, \\ \dot{\omega}_z + k_z\omega_x\omega_y &= T_z/I_z. \end{aligned} \tag{2}$$

In the present analysis, it will be assumed that the torque components are piecewise constant, i.e. the time period of interest can be broken up in a finite number of intervals over which each of the components T_x, T_y, T_z have particular constant values. Thus, also pulsed thrust manoeuvres are included. An important parameter which is directly related to the spin or scan rate ω_z is the nutation frequency ω_n:

$$\omega_n = K\omega_z; \quad K = (k_x k_y)^{1/2}. \tag{3}$$

In addition, the asymmetry ratio k is introduced:

$$k = (k_x/k_y)^{1/2}. \tag{4}$$

Due to the fact that z is either the major or the minor inertia axis both the parameters K and k are well-defined real quantities for any physically meaningful application.

Further simplification of eqns (2) will be achieved after introduction of the nondimensional rotation rates:

$$x = \omega_x/(\omega\sqrt{k}); \quad y = \omega_y\sqrt{k}/\omega; \quad z = \omega_z/\Omega. \tag{5}$$

Here, Ω and ω are scaling constants selected to be representative for the spin and transverse rotation components, respectively. For instance, one may take $\Omega = \omega_z(0)$ and $\omega = |\omega_x(0) + i\omega_y(0)|$ if it is nonzero; otherwise, the latter may be taken to be a representative value for the expected transverse rotation rate. Equations (2) expressed in terms of the variables x, y and z take the form:

$$\begin{aligned} \dot{x} &= T_x/(I_x\omega\sqrt{k}) - (k_y/k)\Omega yz, \\ \dot{y} &= T_y\sqrt{k}/(I_y\omega) + k_x k\Omega xz, \\ \dot{z} &= T_z/(I_z\Omega) - k_z\omega^2 xy/\Omega. \end{aligned} \tag{6}$$

With the aid of the definitions in (3) and (4) one can reduce:

$$k_x/k = k_y k = \begin{cases} +K, & \text{if } I_z \text{ is major,} \\ -K, & \text{if } I_z \text{ is minor.} \end{cases} \tag{7}$$

Therefore, eqns (6) take on different forms depending on whether the major or minor inertia axis is the designated spin or scan axis.

Finally, it appears advantageous to introduce a new time scale τ which is proportional to the total rotation angle about the instantaneous z-axis:

$$\tau(t) = K\Omega \int_0^t z(\mu)\, d\mu. \tag{8}$$

Equations (6) expressed in terms of τ as independent variable can now be written compactly as ($'$ refers to derivatives with respect to τ):

$$\begin{aligned} x'(\tau) &= \xi/z \mp y; \quad y'(\tau) = \eta/z \pm x; \\ z'(\tau) &= (a - bxy)/z. \end{aligned} \tag{9}$$

The upper (lower) signs refer to the case where I_z represents the major (minor) moment of inertia. The constants introduced in eqns (9) are defined as:

$$\begin{aligned} \xi &= T_x/(KI_x\Omega\omega\sqrt{k}); \\ \eta &= T_y\sqrt{k}/(KI_y\Omega\omega); \\ a &= T_z/(KI_z\Omega^2); \\ b &= k_z\omega^2/(K\Omega^2). \end{aligned} \tag{10}$$

The advantage of eqns (9) over the original Euler equations lies in the fact that they are more immediately amenable to a perturbation analysis since only the relative magnitudes of the four constants in eqns (10) need to be analysed for identifying a suitable perturbation parameter. Nevertheless, the system in eqns (9) is still intricately coupled and does not possess any known closed-form solution in the general case.

The constants ξ and η may in general be regarded to be of a similar magnitude, whereas for spin-stabilised spacecraft (i.e. $\Omega \gg \omega$) the constants a and b are, respectively, one and two orders of magnitude (ω/Ω) smaller. On the basis of a consistent scaling policy one may thus write:

$$a = \epsilon\zeta, \quad b = \epsilon^2\kappa, \tag{11}$$

with

$$\zeta = T_z/(KI_z\Omega\omega); \quad \kappa = k_z/K. \tag{12}$$

The small perturbation parameter ϵ appearing here equals the ratio of transverse and spin rotation rates ω/Ω.

For brevity, one may condense the first two equations in (9) by introducing the complex variable $u = x + iy$ with i the imaginary unit:

$$u'(\tau) = c/z \pm iu(\tau), \quad c = \xi + i\eta. \tag{13}$$

The $+$, $-$ signs refer to rotation about major, minor z-axis. The term xy appearing in the equation for z can be expressed as the imaginary part of $u^2/2$. Altogether, the

following extremely compact set of equations has been established:

$$\begin{aligned} u'(\tau) &= c/z \pm iu(\tau), \\ z'(\tau) &= \epsilon[\zeta - \epsilon\kappa\, Im\,(u^2)/2]/z, \\ t'(\tau) &= 1/(K\Omega z). \end{aligned} \tag{14}$$

The time equation is necessary to keep track of the behaviour of the solution as a function of time: this can be accomplished for example by inverting the perturbation solution $t(\tau)$ either directly or iteratively.

Torque-free motion is immediately recovered by putting $c = \zeta = 0$ in eqns (14). For this special case well-known solutions to the Euler equations in the form of elliptic functions are given in the literature, e.g. Wertz[6], Section 16.2.

In the sequel, only the case where z is the major inertia axis will be treated. It is possible to obtain the solution for the alternative case by a simple direct transformation as presented in the Appendix.

2.2 *Perturbation solution for angular rates*

After the relative magnitudes of the forcing terms have been settled a perturbation solution of the form:

$$\begin{aligned} u(\tau) &= u_0(\tau) + \epsilon u_1(\tau) + \epsilon^2 u_2(\tau) + \ldots, \\ z(\tau) &= z_0(\tau) + \epsilon z_1(\tau) + \epsilon^2 z_2(\tau) + \ldots, \\ t(\tau) &= t_0(\tau) + \epsilon t_1(\tau) + \epsilon^2 t_2(\tau) + \ldots, \end{aligned} \tag{15}$$

is postulated. This is a so-called straightforward expansion (e.g. Nayfeh[7], Ch. 2) with short-term validity. After substitution of this expansion into eqns (14) the zeroth-order system is obtained:

$$\begin{aligned} u_0'(\tau) &= c/z_0 + iu_0, \\ z_0'(\tau) &= 0, \\ t_0'(\tau) &= 1/(K\Omega z_0). \end{aligned} \tag{16}$$

On the basis of the initial conditions $u_0(0) = U_0 = X_0 + iY_0$, $z_0(0) = 1$ and $t_0(0) = 0$ one finds the solutions:

$$\begin{aligned} u_0(\tau) &= (U_0 - ic)\exp(i\tau) + ic, \\ z_0(\tau) &= 1, \\ t_0(\tau) &= \tau/(K\Omega). \end{aligned} \tag{17}$$

The zeroth-order solutions for the individual equatorial rotation components $x_0(\tau)$ and $y_0(\tau)$ can readily be derived from $u_0(\tau)$ and they satisfy the relationship:

$$[x_0(\tau) + \eta]^2 + [y_0(\tau) - \xi]^2 = |U_0 - ic|^2. \tag{18}$$

These results show that the u_0 vector describes a circular track within the body's equatorial plane with center at $-\eta + i\xi = ic$ and radius $|X_0 + \eta + i(Y_0 - \xi)|$. In the torque-free case this behaviour is completely consistent with the well-known space and body cone model as described, for instance, by Kaplan[8], Section 2.3. Note also that $\tau = 2\pi$ corresponds precisely to one nutation period as can be seen from the solution for t_0. The effect of the (equatorial) torque components consists effectively of a shift in the position of the u_0 vector's center of rotation as well as in the radius of the circle described. This is related to the displacement of the effective or mean angular momentum position over one spin period under the action of a continuous torque. Only in the case when the initial conditions and torque components are such that $X_0 = -\eta$ and $Y_0 = \xi$ the rotation vector would be fixed in the body frame (at least up to the present level of approximation).

The first-order system of equations is as follows:

$$\begin{aligned} u_1'(\tau) &= -cz_1 + iu_1, \\ z_1'(\tau) &= \zeta, \\ t_1'(\tau) &= -z_1/(K\Omega). \end{aligned} \tag{19}$$

Since now all initial conditions vanish the corresponding solutions can be expressed as:

$$\begin{aligned} u_1(\tau) &= c\zeta[\exp(i\tau) - 1 - i\tau], \\ z_1(\tau) &= \zeta\tau, \\ t_1(\tau) &= -\zeta\tau^2/(2K\Omega). \end{aligned} \tag{20}$$

By expanding $u_1(\tau)$ in its real and imaginary parts the rate components $x_1(\tau)$ and $y_1(\tau)$ can be obtained.

By the nature of the perturbation expansion the dynamical effects have been separated such that the equatorial torque components produce a zeroth-order effect, whereas the spin torque component exhibits itself only in the first-order results. It is evident that this is a consequence of the dominance of the z-axis angular rate over the transverse rates.

The geometrical visualisation of the motion of the $u = u_0 + \epsilon u_1$ vector is similar to that of u_0 with the exception that its center is now moving slowly due to the additional term $-\epsilon c\zeta(1 + i\tau)$ and has a slightly perturbed radius (term $\epsilon c\zeta$).

The second-order system is given by:

$$\begin{aligned} u_2'(\tau) &= c(z_1^2 - z_2) + iu_2, \\ z_2'(\tau) &= -\kappa\, Im(u_0^2)/2 - \zeta z_1, \\ t_2'(\tau) &= (z_1^2 - z_2)/(K\Omega). \end{aligned} \tag{21}$$

In this case the solution is not so straightforward, in particular due to the u_0^2 term which is rather lengthy. It is possible to obtain a closed-form solution for $z_2(t)$ which can be written in short-hand form as:

$$z_2(\tau) = \kappa\,\xi\,\eta\,\tau - \zeta^2\,\tau^2/2 + F(\tau), \tag{22}$$

with

$$\begin{aligned} F(\tau) &= a_1 \sin\tau + (a_2/2)\sin(2\tau) + \\ &\quad + b_1(1-\cos\tau) + b_2[1-\cos(2\tau)]/2, \\ a_1 &= -\kappa\,[\xi(X_0+\eta) - \eta(Y_0-\xi)], \\ a_2 &= -\kappa\,(X_0+\eta)(Y_0-\xi), \\ b_1 &= \kappa\,[\xi(Y_0-\xi) + \eta(X_0+\eta)], \\ b_2 &= -\kappa\,[(X_0+\eta)^2 - (Y_0-\xi)^2]/2. \end{aligned} \tag{23}$$

From this solution expressions for $t_2(\tau)$ and $u_2(\tau)$ can readily be obtained:

$$t_2(\tau) = \{\zeta^2\tau^3/2 - \kappa\,\xi\,\eta\,\tau^2/2 - G(\tau)\}/(K\Omega), \tag{24}$$

with

$$\begin{aligned} G(\tau) &= a_1(1-\cos\tau) + a_2[1-\cos(2\tau)]/4 + \\ &\quad + b_1(\tau-\sin\tau) + b_2[2\tau-\sin(2\tau)]/4. \end{aligned} \tag{25}$$

The solution for $u_2(\tau)$ is given by:

$$\begin{aligned} u_2(\tau) = c\{&3\,i\,\zeta^2\tau^2/2 + (3\,\zeta^2 - i\,\kappa\,\xi\,\eta)(\tau-i) - \\ &- i(b_1+b_2/2) + [(b_1+i\,a_1)/2]\,\tau\cos\tau - \\ &- [(a_1-i\,b_1)/2]\,\tau\sin\tau + \\ &+ (A_2 + i\,b_1/2)\cos\tau + \\ &+ i\,(A_2 - a_1/2)\sin\tau + \\ &+ [(2\,a_2 - i\,b_2)/6]\cos(2\tau) + \\ &+ [(2\,b_2 + i\,a_2)/6]\sin(2\tau)\}, \end{aligned} \tag{26}$$

with integration constant:

$$\begin{aligned} A_2 &= \kappa\,\xi\,\eta - a_2/3 + \\ &\quad + i(3\,\zeta^2 + b_1/2 + 2b_2/3). \end{aligned} \tag{27}$$

The rate components $x_2(\tau)$ and $y_2(\tau)$ can be derived from this result, cf. Van der Ha[9], eqns (46).

This completes the second-order straightforward perturbation solutions for the attitude rates. It is well known[7] that the validity of this approximate result is limited (in the present case over the interval from 0 to $\tau \sim 1/\epsilon$). By repeated rectification or updating of the results after a properly selected interval (e.g. $\tau = k\,2\pi$ with integer k) the validity of the asymptotic solutions can be extended over practically any desired duration.

2.3 *Inversion of time equation*

In order to obtain explicit expressions in terms of time the function $t(\tau)$ as established above must be inverted. Assuming a perturbation expansion for $\tau(t)$ of the form

$$\tau(t) = \tau_0(t) + \epsilon\,\tau_1(t) + \epsilon^2\tau_2(t) + \ldots, \tag{28}$$

one can iteratively solve for the terms $\tau_j(t)$, $j = 0, 1, 2$ by using the known entries of the expansion for $t(\tau)$ as given in eqns (17), (20) and (24):

$$\begin{aligned} \tau_0(t) &= K\Omega t, \\ \tau_1(t) &= \zeta(\kappa\Omega t)^2/2, \\ \tau_2(t) &= \kappa\,\xi\,\eta\,(K\Omega t)^2/2 + G(K\Omega t), \end{aligned} \tag{29}$$

where the function G is defined in eqn (25). This result provides complete flexibility in transforming back and forth between results expressed in the angle τ or time t.

3. ATTITUDE ANGLE EVOLUTION UNDER CONSTANT BODY-FIXED TORQUE

3.1 *Equations of angle evolution in inertial frame*

The attitude evolution itself can be derived from the integration of the results obtained for the rotation rates. A formulation in terms of the so-called Euler parameters is particularly convenient for this purpose as it avoids the singularities inherent in the conventional Euler angles. These parameters are usually defined by means of the instantaneous Euler rotation axis **e** and the corresponding rotation angle W [cf. Morton *et al.*[10], eqns (3)]:

$$\begin{pmatrix} \alpha \\ \beta \\ \gamma \\ \delta \end{pmatrix} = \begin{pmatrix} \cos(W/2) \\ e_1\sin(W/2) \\ e_2\sin(W/2) \\ e_3\sin(W/2) \end{pmatrix}. \tag{30}$$

The relationships between Euler parameters and conventional direction cosine elements are well known[11] and allow to express the Euler parameters in terms of the Euler angles ϕ, θ, ψ (in a 3–1–3 rotation sequence):

$$\begin{aligned} \alpha &= \cos(\theta/2)\cos[(\phi+\psi)/2], \\ \beta &= \sin(\theta/2)\cos[(\phi-\psi)/2], \\ \gamma &= \sin(\theta/2)\sin[(\phi-\psi)/2], \\ \delta &= \cos(\theta/2)\sin[(\phi+\psi)/2]. \end{aligned} \tag{31}$$

The inverse relationships are:

$$\begin{aligned} \phi &= \arctan(\delta/\alpha) + \arctan(\gamma/\beta), \\ \theta &= \arccos[\alpha^2 + \delta^2 - \beta^2 - \gamma^2], \\ \psi &= \arctan(\delta/\alpha) - \arctan(\gamma/\beta). \end{aligned} \tag{32}$$

These equations are important in order to set up the initial conditions for the Euler parameters and for transforming the results back in terms of Euler angles for better visualisation after the integration has been carried out.

The rates of change of the Euler parameters are given by the matrix equation[10].

$$\begin{pmatrix} \dot\alpha \\ \dot\beta \\ \dot\gamma \\ \dot\delta \end{pmatrix} = \frac{1}{2}\begin{bmatrix} 0 & -\omega_x & -\omega_y & -\omega_z \\ \omega_x & 0 & \omega_z & -\omega_y \\ \omega_y & -\omega_z & 0 & \omega_x \\ \omega_z & \omega_y & -\omega_x & 0 \end{bmatrix} \begin{pmatrix} \alpha \\ \beta \\ \gamma \\ \delta \end{pmatrix}. \tag{33}$$

This system can be condensed significantly by employing the complex combinations of Euler parameters (similar to Cayley–Klein parameters):

$$\rho = \alpha + i\beta, \quad \sigma = \gamma + i\delta, \tag{34}$$

with corresponding system of equations:

$$\begin{pmatrix} \dot{\rho} \\ \dot{\sigma} \end{pmatrix} = \frac{i}{2} \begin{bmatrix} \omega_z & \omega_z + i\omega_y \\ \omega_z - i\omega_y & -\omega_z \end{bmatrix} \begin{pmatrix} \rho \\ \sigma \end{pmatrix}. \tag{35}$$

After expressing the rotation rates in terms of the non-dimensional variables introduced in eqns (5) and taking τ of eqn (8) as independent variable one obtains:

$$\begin{pmatrix} \rho'(\tau) \\ \sigma'(\tau) \end{pmatrix} = iw \left\{ \begin{bmatrix} 0 & 1 \\ 1 & 0 \end{bmatrix} + \frac{\epsilon}{z\sqrt{k}} \begin{bmatrix} kx & iy \\ -iy & -kx \end{bmatrix} \right\} \begin{pmatrix} \rho \\ \sigma \end{pmatrix}, \tag{36}$$

with $w = 1/(2K)$. This represents the fundamental system of equations to be formally integrated.

3.2 *Perturbation solution for Euler parameters*

Employing a straightforward perturbation expansion for $\rho(\tau)$ and $\sigma(\tau)$ similar to the ones in eqns (15) one is immediately led to the zeroth-order system of equations by dropping the ϵ term in eqns (36). Its solution is written as:

$$\begin{pmatrix} \rho_0(\tau) \\ \sigma_0(\tau) \end{pmatrix} = \begin{bmatrix} \cos(w\tau) & i\sin(w\tau) \\ i\sin(w\tau) & \cos(w\tau) \end{bmatrix} \begin{pmatrix} A_0 \\ B_0 \end{pmatrix}, \tag{37}$$

with $A_0 = \alpha(0) + i\beta(0)$ and $B_0 = \gamma(0) + i\,\delta(0)$. The torques have thus no effect on the attitude angles in the zeroth-order terms. The first-order system can be expressed in the form:

$$\begin{pmatrix} \rho_1'(\tau) \\ \sigma_1'(\tau) \end{pmatrix} = iw \begin{bmatrix} 0 & 1 \\ 1 & 0 \end{bmatrix} \begin{pmatrix} \rho_1 \\ \sigma_1 \end{pmatrix} + \begin{pmatrix} F_1 \\ G_1 \end{pmatrix}, \tag{38}$$

with

$$\begin{pmatrix} F_1 \\ G_1 \end{pmatrix} = \frac{w}{\sqrt{k}} \begin{pmatrix} ik\,x_0\,\rho_0 - y_0\,\sigma_0 \\ y_0\,\rho_0 - ik\,x_0\,\sigma_0 \end{pmatrix}. \tag{39}$$

The solutions of eqn (38) with vanishing initial conditions follow from the variation-of-parameter formula:

$$\begin{aligned} \rho_1(\tau) &= \int_0^\tau \{F_1(\mu)\cos[w(\tau-\mu)] + \\ &\quad + i\,G_1(\mu)\sin[w(\tau-\mu)]\}\,d\mu, \\ \sigma_1(\tau) &= \int_0^\tau \{iF_1(\mu)\sin[w(\tau-\mu)] + \\ &\quad + G_1(\mu)\cos[w(\tau-\mu)]\}d\mu. \end{aligned} \tag{40}$$

After substitution of the zeroth-order results x_0, y_0, ρ_0 and σ_0 from eqns (17) and (37) into eqns (39) and (40) the following form for the solution can be established:

$$\begin{aligned} \rho_1(\tau) &= C^+\cos(w^+\tau) - C^-\cos(w^-\tau) + \\ &\quad + S^+\sin(w^+\tau) + S^-\sin(w^-\tau) - \\ &\quad - D\cos(w\tau) + (T - S)\sin(w\tau), \\ \sigma_1(\tau) &= i\,S^+\cos(w^+\tau) + i\,S^-\cos(w^-\tau) - \\ &\quad - i\,C^+\sin(w^+\tau) + i\,C^-\sin(w^-\tau) - \\ &\quad - i\,T\cos(w\tau) - i(C + D)\sin(w\tau). \end{aligned} \tag{41}$$

The frequencies $w^\pm$ denote $w \pm 1$ and the constants appearing here are defined as:

$$\begin{aligned} C^\pm &= C_1^\pm/(2w \pm 1); \\ S^\pm &= S_1^\pm/(2w \pm 1); \\ C &= (i\,\xi\,A_0 - k\,\eta\,B_0)/\sqrt{k}; \\ S &= (i\,k\,\eta\,A_0 + \xi\,B_0)/\sqrt{k}; \\ D &= C^+ - C^-; \\ T &= S^+ + S^-; \end{aligned} \tag{42}$$

with

$$\begin{aligned} C_1^\pm &= w(k \pm 1)\{i\,A_0(Y_0 - \xi) \pm \\ &\quad \pm B_0(X_0 + \eta)\}/(2\sqrt{k}); \\ S_1^\pm &= w(k \pm 1)\{i\,A_0(X_0 + \eta) \mp \\ &\quad \mp B_0(Y_0 - \xi)\}/(2\sqrt{k}). \end{aligned} \tag{43}$$

It may be noted that the equatorial torque components appear in this first-level of approximation. The axial torque component will enter the second-order solution via the first-order rate solution.

The second-order system for $\rho_2(\tau)$ and $\sigma_2(\tau)$ takes the same form as in eqn (38) with considerably more complicated forcing terms:

$$\begin{pmatrix} F_2 \\ G_2 \end{pmatrix} = \frac{w}{\sqrt{k}} \begin{pmatrix} ik(x_0\,\rho_1 + x_1\,\rho_0 - x_0\,\rho_0\,z_1) - (y_0\,\sigma_1 + y_1\,\sigma_0 - y_0\,\sigma_0\,z_1) \\ y_0\,\rho_1 + y_1\,\rho_0 - y_0\,\rho_0\,z_1 - ik(x_0\,\sigma_1 + x_1\,\sigma_0 - x_0\,\sigma_0\,z_1) \end{pmatrix}. \tag{44}$$

The solutions can also formally be written in the form of eqns (40). In fact, explicit expressions have been established in terms of some 20 different integrals. These solutions are extremely lengthy and have been spelled out in an internal ESA report (Van der Ha[9]). For reasons of brevity they are omitted here. In many practical cases (especially when $\zeta = 0$) the first-order results would

already be sufficiently accurate so that the elaborate coding of the second-order angular evolution may be avoided. In this connection it may be mentioned that the accuracy of the solutions can readily be enhanced by a rectification of the results at regular intervals.

4. APPLICATIONS OF THE THEORY

The approximate solutions for the attitude motion established above are of considerable practical importance as they allow a quick evaluation of a spacecraft's attitude response to a variety of disturbing and/or control torques. Of particular importance is the fact that the theory is not restricted to symmetric rigid bodies but includes the asymmetry effect through the κ terms without approximation. This so-called "self-excited asymmetric rigid body" problem has received relatively little attention in the literature so far. Nevertheless, it possesses unique dynamic characteristics whose understanding is vital for safe satellite manoeuvre operations as will be illustrated below.

4.1 *Application to spin-stabilised spacecraft*

When ESA's spin-stabilised satellite GEOS-1 was to undergo a 45 min orbit manoeuvre by means of an axial thruster burn in may 1979 there appeared to exist little reason for concern. In fact, a similar manoeuvre of 3 min duration had already successfully been performed two years earlier. There were however two apparent differences between the conditions surrounding these two manoeuvres. One of these was thought to be important, namely the fact that in the meantime the 20 m radial wire booms had been deployed. The other difference concerned the spin rate which was only 11 rpm compared to 96 rpm prior to the first manoeuvre. It could not *a priori* be excluded that spin rate variations would induce boom oscillations. In order to analyse the effect on the booms a computer simulation based on the best available nonlinear model was carried out. Contrary to the outcome of a simpler linear model the simulations predicted a complete despin (and loss of the satellite due to boom slackness) after just 5 min! When these predictions were analysed in more detail it became clear that the nonlinear rate coupling effect inherent in the Euler equations in conjunction with the comparatively low spin rate rather than any boom dynamics was responsible for the despin. A subsequent verification manoeuvre of small duration confirmed the correctness of the quantitative predictions. A first-hand account of this narrow-escape satellite saga is given by Boland and Janssens[5].

The rate coupling effect referred to here may introduce a spin-up or -down due to the net cumulative effect of the forcing term $-k\ \omega_x\ \omega_y$ in the third Euler equation [eqns (2)]. This is seen explicitly in eqn (22) which in the absence of the axial torque component and apart from periodic terms can be expressed as $z_2 = \kappa\ \xi\ \eta\ \tau$. On the basis of the definition of the symbols given in eqns (5), (10) and (12) along with the expansion of τ in terms of t given in eqns (29) this result can be rewritten in the original dynamical parameters as:

$$\Delta\omega_z(t) = \frac{(I_x - I_y)\ T_x\ T_y\ t}{(I_z - I_y)(I_z - I_x) I \Omega^2} = \\ = J\ T_x\ T_y\ t/\Omega^2, \quad (45)$$

with inertia parameter J defined by this equation. This expression is consistent at least in the case of a small spin change with a formula given in [5], eqn (19), which was derived on the basis of energy considerations. The nonintuitive change in spin rate is brought about by the fact that (in average over a nutation cycle) the equatorial torque vector has a nonvanishing component along the angular momentum vector thereby changing its magnitude. Equation (45) indicates that no spin change occurs for a symmetrical satellite ($I_x = I_y$) or if either T_x or T_y vanishes, i.e. when the axial thruster is positioned on one of the principal axes.

In the case of GEOS-1 the lower axial thruster is located 0.725 m away from the spin axis at 40° from the principal x-axis. It was expected to produce a 7 N thrust for the orbit manoeuvre under consideration. The inertia parameter J in eqns (45) amounts to 8.914×10^{-5} (kgm^2)$^{-1}$ where the contributions of the wire booms have been incorporated in the way proposed in eqn (28) of [5]. Table 1 provides the comparison of the predicted and actually observed spin-downs during the two verification manoeuvres. The last two columns are reproduced from [5]. It is seen that the agreement of the models with the observations is extremely good.

Other spin-stabilised ESA spacecraft which may be subjected to the same phenomenon are the METEOSAT-1 and 2 satellites. Since, however, their operational spin rate is around 100 rpm it is evident from eqn (45) that the rate coupling effect is much less pronounced than in the case of GEOS. Using typical inertia values one finds a value for the inertia parameter J in eqn (45) of the order of 10^{-4} (kgm^2)$^{-1}$. For typical thrust levels this results in a spin-down of only 0.03–0.08 rpm per minute of thrust (for the nominal axial -1 thruster; the backup thruster would produce a similar spin-up). The spin-down due to jet damping (caused by fuel displacement to thruster location) can be shown to be of a magnitude already three times larger. In fact, thrust misalignments also introduce larger spin changes. Therefore, it can be concluded that the coupling effect has comparatively minor implications for this class of fast-spinning satellites.

Table 1. Summary of observed and predicted spin-downs during GEOS-1 verification manoeuvres

manoeuvre number	duration (sec)	initial spin(rpm)	actual $\Delta\omega_z$(rpm)	predicted $\Delta\omega_z$ (rpm)		
				Eq.(45)	computed	analytical
1	82	10.97	-0.61	-0.67	-0.61	-0.72
2	181	11.00	-1.47	-1.47	-1.50	-1.73

4.2 *Application to HIPPARCOS attitude motion*

The perturbation solutions presented here have also shown to be extremely valuable in predicting the attitude drift motion of a slowly scanning asymmetric rigid body under a body-fixed perturbing torque. The application at hand concerns ESA's astrometry satellite HIPPARCOS which is foreseen to be launched in 1988. Its scan axis is normal to the plane formed by two telescope arms which are separated by a 58° basic angle. The nominal scan rate is extremely slow: $\omega_z = 168.75$ deg/h. Stars appearing in each of the two telescopes fields of views are projected in one common focal plane by means of a beam combining mirror. The close proximity (within the payload) of stars which are actually separated by about 58° on the celestial sphere is essential for achieving the milli-arcsec level astrometric accuracies by an elaborate data processing of all measurements. A general overview on the HIPPARCOS mission's principles and objectives can be found in Schuyer[12]. An account with emphasis on attitude control aspects is given by Vilain and Harris[13].

During the initialisation of its payload the satellite's scan axis is roughly pointing in the direction to the Sun. The scan rate is kept close to its nominal value by a control loop incorporating a z-axis gyro rate sensor and torques provided by the cold gas reaction control system. The dominant perturbing torque in this configuration is due to the z-axis gyro's reaction to the imposed scan motion. It may be recalled that a gyro having its input axis along the z-axis must have its angular momentum vector somewhere in the equatorial plane with the consequence that the imposed scan precession about the z-axis will generate a reaction torque normal to both angular momentum and z-axis direction. This body-fixed torque vector lies in the satellite's equatorial plane and has a magnitude of 11 micro-Newton in the present application.

In order to establish complete three-axis knowledge of the spacecraft's orientation the inertial pointing directions of the telescopes will be determined by analysing the star patterns observed in the payload's Star Mapper. The recognition of these patterns is considerably complicated by the fact that stars from both field of view directions are crossing the 40 arcmin wide Star Mapper slits. The first task in the recognition process would therefore consist of a separation of the observed star patterns according to their fields of view. This may be accomplished by a careful comparison of two patterns separated by a time interval of 20.6 min corresponding to the basic angle scan of 58°. On the basis of the assumption that there exists a reasonable overlap between the scanned strips over this time interval it should be feasible to distinguish that part of the star pattern which is completely identical in the two compared patterns: these common stars must belong to the "following" field of view of the most recent observation and to the "preceding" direction 20.6 min earlier. The remaining stars in the common strip would then belong to the respective alternative fields of view. A detailed account on the feasibility of the star pattern recognition briefly discussed here is provided in an internal ESA report[14].

From the considerations raised above it is evident that the extent of the overlap region after a 20.6 min basic angle scan should be made as large as possible in order to facilitate the star pattern separation task. Since the direction of the gyro reaction torque within the equatorial plane can be selected at will there is room for optimisation. Thus, a parametric search for the optimal torque direction has been carried out using the results of the theory presented above. As HIPPARCOS is scanning along its minor inertia axis the transformation outlined in the Appendix was necessary. The perturbation solutions up to first-order terms as well as a RUKUT 4 nu-

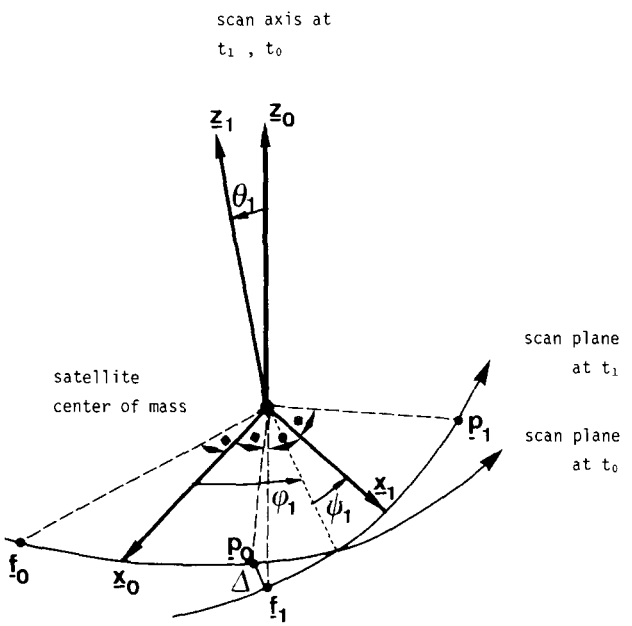

Fig. 1. Visualisation of shift Δ between preceding field of view at t_0 and following field of view at t_1.

Table 2. Summary of shift in field of view directions Δ in arcmin for torque directions between $-30°$ and $20°$

initial ω_x , ω_y (deg/hr)		torque direction α in equatorial plane					
		-30°	-20°	-10°	0°	10°	20°
0	0	26	15	2	-10	-22	-33
2	1	8	-3	-16	-28	-40	-51
-2	1	4	-7	-20	-32	-44	-55
2	-1	48	36	24	12	0	-11
-2	-1	44	32	20	8	-4	-15

merical integration routine were coded in Basic on a 16K homecomputer. The results indicated acceptable agreement, i.e. 5–7 common digits for the rates and 3–5 for the Euler parameters over the basic angle interval. An additional comparison with a different analytical perturbation solution confirmed the validity. The analytical solution was about 5 times faster in CPU time than the numerical.

Finally, the field of view shift after one basic angle scan will be analysed. The bisector of the two field of view directions is taken as the x-axis of the body-fixed reference frame. For convenience the inertial frame is thought to be aligned with the body frame at time $t = 0$. The initial Euler parameters are therefore $\alpha(0) = 1$; $\beta(0) = \gamma(0) = \delta(0) = 0$. After an interval of $t_1 = 20.6$ min corresponding to the basic angle scan the prevalent Euler parameters $\alpha(1)$–$\delta(1)$ are provided by the perturbation solutions above. The corresponding Euler angles $\phi(1)$, $\theta(1)$ and $\psi(1)$ can be calculated from eqns (32). The shift in pointing direction of the following telescope at t_1, i.e. $\mathbf{f}(1)$, relative to that of the preceding field of view direction at t_0, i.e. $\mathbf{p}(0)$, is given by (cf. Fig. 1):

$$\Delta \cong \sin\theta(1)\sin[\psi(1) - 29°] = 2\{c(\beta\delta - \alpha\gamma) - s(\alpha\beta + \gamma\delta)\}_{t=t_1}, \tag{46}$$

where $c = \cos(29°)$ and $s = \sin(29°)$. (Note that 29° is half of basic angle.)

The results of 6 different torque directions α between $-30°$ and $20°$ are summarised in Table 2. The first row refers to the case where the initial pointing is completely at rest, whereas the other four rows represent worst-case initial rates. (These initial conditions correspond to the residual deadband motion remaining after switch-off of the Sun-pointing control loop.) When applying equal weights to each of the 5 cases presented in Table 2 one finds that the overall optimal value of α is around $-8°$. The corresponding worst-case shift in field of view would be about 22 arcmin so that the remaining overlap is expected to be slightly less than half of the 40 arcmin wide Star Mapper slits. This is expected to be adequate for a successful star pattern separation.

5. CONCLUDING REMARKS

Perturbation solutions for the attitude rates and angles have been established for a rigid body with arbitrary inertia parameters subjected to constant body-fixed torque components. The perturbation expansions have been carried up to second-order in terms of a small parameter designating the ratio between a representative transverse rotation rate and spin or scan rate. This condition essentially amounts to a small nutation angle so that the results should be useful for any application where one axis exhibits a clearly dominant rotation rate. The attitude angles can be derived from a set of redundant Euler parameters which are not hampered by the singularities inherent in a formulation in terms of conventional Euler angles.

The approximate analytical solutions derived here should have wide practical applicability as they allow a quick evaluation of a satellite's attitude response to a variety of disturbing or control torques. It has been shown that the results are capable of correctly predicting the intricate dynamics of asymmetric spin-stabilised spacecraft. The potentially disastrous rate coupling effect on the GEOS spacecraft should have taught us clearly that rigid-body dynamics may still have a few more secrets in store for us. Simple but realistic analytical models could be extremely useful for discovering and understanding these dynamical surprises.

Furthermore, it has been shown that already the first-order perturbation results (implemented on a homecomputer) are able to predict the HIPPARCOS attitude drift under a gyro-induced disturbance torque to sufficient accuracy. In this application the nominal scan rate is only 168.75 deg/h.

As for future applications it appears that realistic compact analytical expressions modelling the attitude evolution should become important in onboard attitude control software, e.g. calculation of planned manoeuvre effects or control loop adaptation on the basis of observed disturbance torques.

REFERENCES

1. F. Janssens, Nutation of a symmetric rigid body under continuous thrusting; application to METEOSAT-2, *ESTEC* Working Paper 1247, July 1980.
2. E. Leimanis, *The General Problem of the Motion of Coupled Rigid Bodies about a Fixed Point*, Springer Verlag, Berlin (1965).
3. R. Grammel, Der selbsterregte unsymmetrische Kreisel, *Ingenieur-Archiv*, **22**, 73–97 (1954).
4. J. M. Longuski, Solution of Euler's equations of motion and Eulerian angles for near symmetric rigid bodies subject to constant moments, *AIAA Paper* 80-1642 (Aug. 1980).
5. Ph. Boland and F. Janssens, The GEOS-1 dynamic experiment, *ESA J.*, **3**, 265–280, 1979.

6. J. R. Wertz (ed.), *Spacecraft Attitude Determination and Control*, Reidel, Dordrecht, Holland (1978).
7. A. H. Nayfeh, *Perturbation Methods*, Wiley, New York (1973).
8. M. H. Kaplan, *Modern Spacecraft Dynamics & Control*, Wiley, New York (1976).
9. J. C. Van der Ha, Perturbation solution for attitude motion under body-fixed torques, *ESOC*, OAD Working Paper 242 (Jan. 1984).
10. H. S. Morton, J. L. Junkins and J. N. Blanton, Analytical solutions for Euler parameters, *Celest. Mechan.* **10**, 287–301 (1974).
11. C. Grubin, Derivation of the quaternion scheme via the Euler axis and angle, *J. Spacecraft Rockets*, **7**, 1261–1263 (1970).
12. M. Schuyer, HIPPARCOS—A European astrometry satellite mission objectives, technical issues and approaches, *Space 2000*, Ed. by L. G. Napolitano, AIAA, New York, 1983, pp. 355–372.
13. D. Vilain and R. S. Harris, Attitude determination and control of the HIPPARCOS satellite, *Amer. Astronaut. Soc.*, Paper AAS-84-005, Feb. 1984.
14. J. C. Van der Ha and P. De Broeck, Feasibility study of HIPPARCOS initial star pattern recognition, *ESOC*, OAD Working Paper 220, March 1983.

APPENDIX: SPIN OR SCAN ABOUT MINOR INERTIA AXIS

The mathematical formulation presented above was based on the assumption that the designated spin or scan axis (i.e. z-axis) is the major axis of inertia. In the alternative case when the z-axis represents the minor-axis of inertia the lower signs in eqns (9) and (14) must be taken and the corresponding perturbation solution will be different from the one given.

It is possible, however, to immediately transform the solution presented above to the one valid for the case of rotation around the minor axis. Thereto one makes the substitution:

$$\bar{y} = -y; \quad \bar{\eta} = -\eta; \quad \bar{b} = -b. \tag{A1}$$

This change of variables transforms one system of eqns (9) into the other and allows to employ the given solutions also for the minor axis rotation after incorporating the appropriate sign changes. The transformation of eqn (A1) can be accommodated in eqns (14) by replacing κ by $-\bar{\kappa}$; u by $\bar{u} = x + i\bar{y} = x - iy$ and c by $\bar{c} = \xi - i\eta$. The initial condition for y appearing implicitly (in U_0) must be transformed in the same manner. By this change of variables the validity of the given solutions can thus quickly be extended also to this important alternative case.